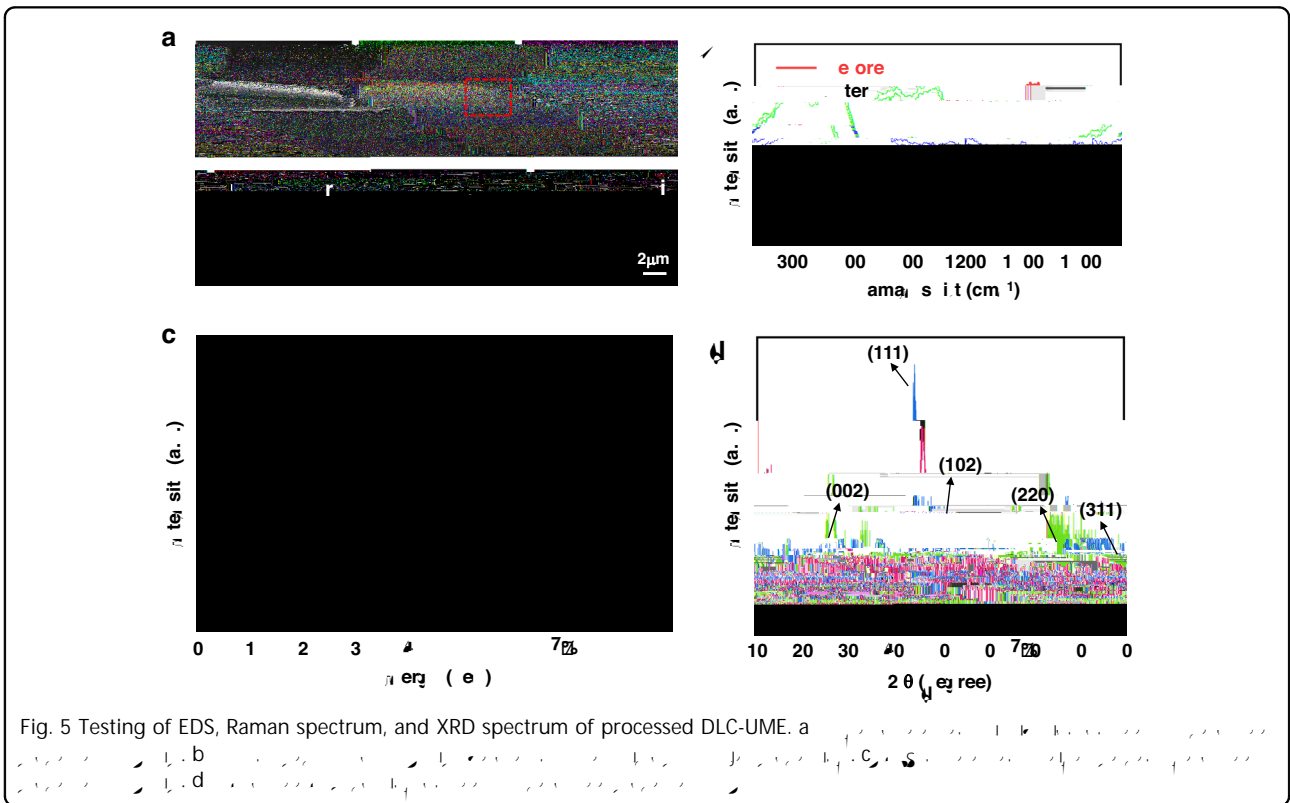
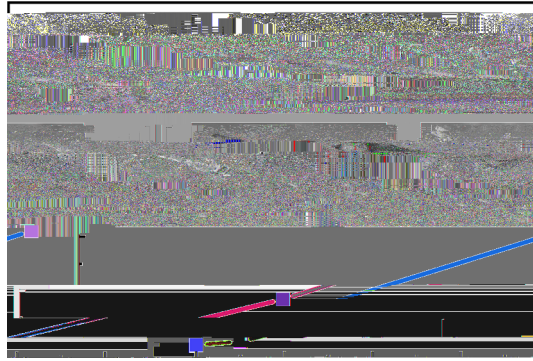


length of 6 m was fi

properties and is compatible with MEMS processes, with good detection repeatability, electrochemical stability, biocompatibility, and targeted detection ability for intracellular pH^{15,48}. The IrOx layer on the UME tip presented an earthworm-like nanowire structure, increasing the surface area of the UME detection point and reducing impedance (Fig. 3b and c). Due to the simultaneous reversible reactions between Ir³⁺ and Ir⁴⁺ states⁴⁹, the capacitance of the UME increases and the ability of UME to transfer charges within cells is enhanced, thereby increasing detection sensitivity and signal-to-noise ratio. From the cross-section of the UME tip, the thickness of the DLC layer covering the IrOx was consistent with the expected thickness of about 400 nm (Fig. 3d). The DLC layer had a dense nanoparticle structure (Fig. 3e and f), which enabled good coverage of the the UME surface and contributes to the effective protection of the UME.



26.35, 15.27, 32.47, 24.14, 0.39, 1.38, respectively (Fig. 5c). Moreover, the atomic ratio of Ir to O is 4.83: 27.30. The relative content of each element is influenced by the thickness and distribution of each coating from the outside to the inside of the UME. By comparing the distribution and density of C atoms in the red box area of Fig. 5a with other elements, it can be concluded that the DLC coating at the UME tip has been successfully

removed, and other coatings were still intact (Fig. 5a). The surface of the untreated UME tip was coated with DLC film with typical mixed structure of sp^2 and sp^3 carbon⁵⁰, and its Raman spectrum consisted of the typical D-peak of 1350 cm^{-1} and G-peak of 1580 cm^{-1} , while the presence of D-peak or G-peak was not detected at the UME tip after microplasma jet processing due to the complete removal of the DLC coating on the UME surface (Fig. 5b).

Then, five diffraction peaks were found at 2θ values of 26.2°, 44.1°, 51.6°, 75.4° and 89.1° in the XRD spectra of the processed UME (Fig. 4d). It can be observed that the XRD spectra was dominated by three intense peaks located at $2\theta \sim 44.1^\circ$, 75.4° and 89.1° , which can be identified by the reflection of diamond (111), (220) and (311) planes⁵⁰. The peaks located at $2\theta \sim 26.2^\circ$ and 51.6° were corresponding to the graphite (002) and (102), respectively⁵¹. In a word, the DLC coating on the surface of the processed UME was composed of a certain proportion of diamond graphite with high crystallinity. Furthermore, the growth status of the cells with the UME placed within seven days was as good as that of the control group within the seven days of testing, which indicated the DLC-UME has good biocompatibility (Fig. S1).

Electrochemical characterization of DLC-UME

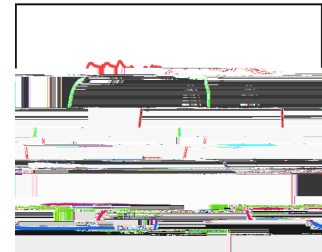
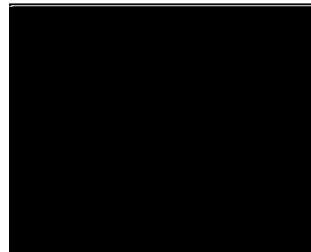
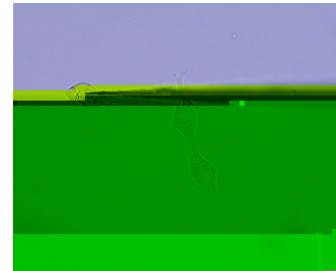
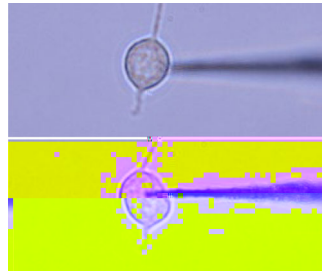
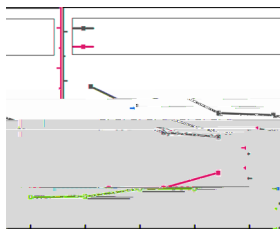
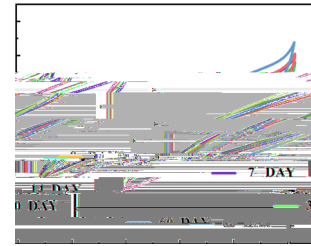
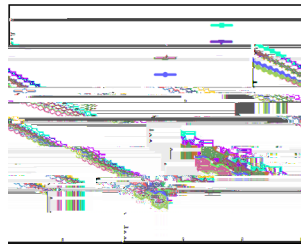
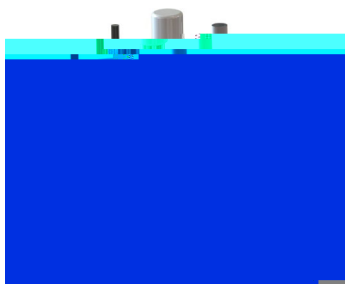
The electrochemical performance was tested using a micromanipulator to clamp the DLC-UME as the working electrode (WE), an Ag/AgCl electrode as the reference electrode (RE), and a Pt electrode as the counter electrode (CE) (Fig. 6a). Accelerated aging testing has been used to evaluate the intracellular lifespan of UMEs⁵². Placing the UME in a high-temperature environment will accelerate the chemical reaction of the UME surface coatings to accelerate its degradation, thus evaluating the long-term stability of the UME in a short period of time⁵³. A commonly used formula is Eq. S1⁴⁷. In our work, the reference temperature was set to 37 °C suitable for HT22 cells growth and the ambient temperature was kept at 60 °C for an accelerated aging factor of 4.9 according to Eq. S1 by placing the beaker with electrodes on a hot plate. The impedance frequency response curves and CV curves of the DLC-UME were recorded with the accelerated aging time of 0 h, 34 h, 68 h, 147 h, and 294 h, corresponding to approximately 0 days, 7 days, 14 days, 30 days, and 60 days, respectively (Fig. 6b, c). As the UME ages, the impedance slowly decreased at the frequency of 1 kHz, and the limit current slowly increased at the applied potential of 0.8 V. The changes in impedance and current within 60 days were very small (Fig. 6d).

The electrochemical performance of the UME was still stable after 60 days, which may be attributed to the good electrochemical stability of the DLC coating and the modification of the DLC coating by microplasma jet. With the introduction of O-containing functional groups in the microplasma jet, sp_2 bonding was broken, reducing the degree of graphitization of DLC^{54,55}. O atoms adsorbed at defect sites in DLC material to form various O-containing functional groups and more sp_3 carbon appears, resulting in a decrease in conductivity and an increase in internal Ohmic resistance of the DLC coating⁵⁶, which may improve the compactness and the electrochemical shielding ability of the DLC coating and contribute to the effective protection of the UME.

Electrophysiological recordings of intracellular signals of neurons

Electromotive force (EMF), which represents the potential difference between the RE and the WE at zero current, which can be used to characterize the intracellular potential response⁵⁷. The DLC-UME was inserted into the cultured HT22 cells, and the cell membrane underwent slight deformation (Fig. 6e). Then, the UME was sequentially implanted into three different cells for the signal recording (Fig. 6f). Equivalent circuit diagram of the UME inserted into the cytoplasm in a dual electrode system is shown in Fig. 6g, where R_e represents electrode resistor, R_m represents cell membrane resistor, R_b represents bulk solution resistor, C_e represents electrode capacitor, and C_m represents cell membrane capacitor, which is used to simplify complex behaviors inside and outside cells¹⁵.

Intracellular pH value is closely related to cellular metabolism, carcinogenesis, and apoptosis, which is crucial for a deeper understanding and diagnosing diseases. The corresponding relationship between pH and EMF, named the E-pH response sensitivity, was measured to be approximately 34ly



culture medium in a short period of time. Results above demonstrated that the DLC-UME was sensitive to pH changes and had good reversibility and stability in intracellular recording.

Conclusion

This work presented a method of selectively etching UME tip protective coatings using microplasma jet, enabling controllable exposure of tip functional coatings to achieve effective insulation and interference shielding. DLC coating was chosen as a protective layer for the sharp UME for the first time. By determining the optimal interaction mode between microplasma jet and UME and analyzing the changes in the microscopic morphology of

UME tips with processing time during the removal of protective layer materials, the exposed tip length was precisely controlled down to the submicron scale. Then, we evaluated the phase composition and lattice orientation of the DLC film deposited on the UMEs, analyzed the elemental composition and compositional changes after microplasma jet processing and verified through a one-week biocompatibility control experiment that the DLC-UME had no adverse effects on the normal growth of neuron cells. Finally, electrochemical aging tests and real-time single-cell intracellular pH detection experiments provided evidence that the DLC-UME with effective tip protection processed by microplasma jet held the potential to enable the precise and long-term detection of

intracellular signals. Our work provides a new method for the external effective protection of UMEs in single-cell analysis, which can expand more available materials as the protective layers of UMEs, improve the fidelity and long-term stability of single-cell recording and contribute to the scientific research on accurate diagnosis and monitoring of brain diseases in the future.

Acknowledgements

1. [https://doi.org/10.1002/anie.201910000](#), *Angew. Chem., Int. Ed.* **60**, 1-5 (2021).
2. [https://doi.org/10.1039/C9SC02000A](#), *Chem. Sci.* **10**, 1000-1005 (2019).